Biogeosciences Discuss., https://doi.org/10.5194/bg-2018-11
Manuscript under review for journal Biogeosciences
Discussion started: 16 January 2018

Interactive effects of seawater carbonate chemistry, light intensity and nutrient availability on physiology and calcification of the coccolithophore *Emiliania huxleyi*

Yong Zhang[1], Feixue Fu[2], David A. Hutchins[2], and Kunshan Gao[1]

[1]State Key Laboratory of Marine Environmental Science, Xiamen University, Xiamen, China

[2]Department of Biological Sciences, University of Southern California, Los Angeles, California

Running head: *carbonate chemistry,* Emiliania huxleyi, *light, nutrients*

Correspondence to: Kunshan Gao (ksgao@xmu.edu.cn)

Keywords: calcification; CO_2; coccolithophore; growth; light; nutrient; photosynthesis

Biogeosciences Discuss., https://doi.org/10.5194/bg-2018-11
Manuscript under review for journal Biogeosciences
Discussion started: 16 January 2018

Abstract. Rising atmospheric carbonate dioxide (CO_2) levels lead to increasing CO_2 concentration and declining pH in seawater, as well as ocean warming. This enhances stratification and shoals the upper mixed layer (UML), hindering the transport of nutrients from deeper waters and exposing phytoplankton to increased light intensities. In the present study, we investigated combined impacts of CO_2 levels (410 μatm (LC) and 925 μatm (HC)), light intensities (80–480 μmol photons m^{-2} s^{-1}) and nutrient concentrations [101 μmol L^{-1} dissolved inorganic nitrogen (DIN) and 10.5 μmol L^{-1} dissolved inorganic phosphate (DIP) (HNHP); 8.8 μmol L^{-1} DIN and 10.5 μmol L^{-1} DIP (LN); 101 μmol L^{-1} DIN and 0.4 μmol L^{-1} DIP (LP)] on growth, photosynthesis and calcification of the coccolithophore *Emiliania huxleyi*. HC and LN synergistically decreased growth rates of *E. huxleyi* at all light intensities. High light intensities compensated for inhibition of LP on growth rates at LC, but exacerbated inhibition of LP at HC. These results indicate that the ability of *E. huxleyi* to compete for nitrate and phosphate may be reduced in future oceans with high CO_2 and high light intensities. Low nutrient concentrations increased particulate inorganic carbon quotas and the sensitivity of maximum electron transport rates to light intensity. Light-use efficiencies for carbon fixation and calcification rates were significantly larger than that of growth. Our results suggest that interactive effects of multiple environmental factors on coccolithophores need to be considered when predicting their contributions to the biological carbon pump and feedbacks to climate change.

Biogeosciences Discuss., https://doi.org/10.5194/bg-2018-11
Manuscript under review for journal Biogeosciences
Discussion started: 16 January 2018

1 Introduction

Anthropogenic emission of CO_2 is taken up by the oceans, decreasing pH of seawater and resulting in ocean acidification (OA) (Caldeira and Wickett, 2003). On the other hand, rising atmospheric CO_2 also leads to global and ocean warming, which enhances water column stratification and shoals the upper mixed layer (UML) (Wang et al., 2015). This exposes phytoplankton dwelling in the UML to higher light intensities (Gao et al., 2012; Hutchins and Fu, 2017). In addition, enhanced stratification reduces the transport of nutrients from deep oceans to the UML (Behrenfeld et al., 2006), which reduces the nutrient concentrations in the UML.

Coccolithophores take up CO_2 and/or HCO_3^- from media for carboxylation, and use HCO_3^- for calcification which produces coccoliths. Calcification processes generate CO_2 due to production of protons, which counteracts with photosynthetic CO_2 fixation, and therefore influencing CO_2 influx into the oceans (Rost and Riebesell, 2004). Growth rate, particulate organic (POC) and inorganic carbon (PIC) production rates of *Emiliania huxleyi*, the most abundant calcifying coccolithophore species, usually display optimum responses to a broad range of CO_2 concentration, with growth, POC and PIC production rates increased, decreased or unaffected by rising CO_2 treatments (Langer et al., 2009; Richier et al., 2011; Bach et al., 2015; Jin et al., 2017). Increased light levels could counteract the negative effects of rising CO_2 on calcification in *E. huxleyi* when grown under natural fluctuating sunlight (Jin et al., 2017). Differences in sampling locations, experimental setups, and deviations in the

Biogeosciences Discuss., https://doi.org/10.5194/bg-2018-11
Manuscript under review for journal Biogeosciences
Discussion started: 16 January 2018

68 measuring methods can generally be responsible for the differential responses of
69 growth, POC and PIC productions to rising CO_2 in *E. huxleyi* (Meyer and Riebesell,
70 2015).

71 POC production as well as growth rates usually increase with elevated light levels,
72 level off at saturated light levels and decline at inhibited high light levels in
73 cocolithophores (Zhang et al., 2015; Jin et al., 2017). Reduction in pigment content
74 and effective photochemical quantum yield ($F_v^{'}/F_m^{'}$) are characteristics of
75 photo-acclimation (Geider et al., 1997; Gao et al., 2012). At low light intensity, the
76 ratio of light-harvesting protein to photosystem II (PSII) reaction center proteins is
77 large, which facilitates *E. huxleyi* to absorb more energy. At high light intensity, the
78 ratio of photo-protection proteins to PSII reaction center proteins is large, which could
79 protect *E. huxleyi* against damage caused by high light intensities (Mckew et al.,
80 2013).

81 Nitrogen is required for the biosynthesis of proteins and other macromolecules,
82 including chlorophyll (Riegman et al., 2000). Phosphorus is required for the synthesis
83 of nucleic acids, ATP, and phospholipids in cell membranes (Shemi et al., 2016). Due
84 to source limitation, decreased nutrient concentrations usually reduce growth and
85 photosynthetic carbon fixation rates (Cloern et al., 1999; Kim et al., 2007; Harrison et
86 al., 2008). Nevertheless, low nutrient concentrations often enhance the PIC quotas of
87 *E. huxleyi*. This is due to the fact that low nutrient concentrations hold the cells in the
88 G1 cell cycle phase where calcification occurs (Müller et al., 2008). A recent
89 proteome study on *E. huxleyi* also shows that nutrient limitation arrests cell cycling

Biogeosciences Discuss., https://doi.org/10.5194/bg-2018-11
Manuscript under review for journal Biogeosciences
Discussion started: 16 January 2018

(McKew et al., 2015). At molecular levels, nitrate or phosphate limitations down-regulate expression of genes involved in cell cycling, RNA and protein synthesis in *E. huxleyi* (Rokitta et al., 2014, 2016).

Recently, several studies investigated interactive effects of rising CO_2 and light intensity on physiological rates of coccolithophores (Feng et al., 2008; Jin et al., 2017). Zhang et al. (2015) reported that at 50–800 μmol photons m^{-2} s^{-1}, rising CO_2 levels decreased the maximum growth rate, POC production rate and PIC production rate of *Gephyrocapsa oceanica*. At low light levels, coccolithophores increase CO_2 uptake to compensate for inhibition of HCO_3^- uptake on photosynthesis, while at high light intensity they don't increase CO_2 uptake (Kottmeier et al., 2016). Under natural solar radiation, Jin et al. (2017) reported that rising CO_2 levels increased the growth and POC production rates of *E. huxleyi* at high sunlight levels. Interaction of rising CO_2 with light appears to affect differentially coccolithophores when grown under different experimental setups.

Some previous studies have examined the effects of rising CO_2 and nutrient concentrations on the physiology of *E. huxleyi* (Sciandra et al., 2003; Borchard et al., 2011; Engel et al., 2014; Müller et al., 2017). Low nitrate or low phosphate concentrations increased POC and PIC quotas in *E. huxleyi*, and these increases were much less at high CO_2 than at low CO_2 levels (Matthiessen et al., 2012; Rouco et al., 2013). In addition, rising CO_2 levels decreased growth rates at high phosphate concentration, though it did not affect growth rates at low phosphate concentration (Matthiessen et al., 2012). These studies indicate that fitness-relevant traits of *E.*

112 *huxleyi* may be altered in future high-CO_2 and low-nutrient oceans.

113 Recently, researchers have paid increasing attentions to combined effects of
114 multiple stressor on marine phytoplankton (Brennan and Collins, 2015; Boyd et al.,
115 2016; Hutchins and Fu, 2017), considering the fact that phytoplankton cells are
116 simultaneously exposed to physical and chemical factors. In addition, physiological
117 responses of phytoplankton to one environmental factor may be synergistically,
118 antagonistically or neutrally affected by others (Tong et al., 2016; Müller et al., 2017).
119 Even across a broad range of CO_2 concentrations, optimal CO_2 levels and maximal
120 values for growth rate, photosynthetic carbon fixation rate and calcification rate are
121 modulated by temperature and light intensity (Sett et al., 2014; Zhang et al., 2015).

122 Under chemostat cultures, rising CO_2 levels were found to increase the POC quotas
123 of a non-calcifying strain of *E. huxleyi* (PML 92A) and a calcifying strain of *E.*
124 *huxleyi* (PML B92/11) at low nutrient concentration and high light intensity
125 (Leonardos and Geider, 2005; Borchard et al., 2011). However, relatively few studies
126 have observed the interactive effects of multiple environmental factors on
127 physiological rates of coccolithophores. To investigate responses of the calcifying *E.*
128 *huxleyi* strain PMLB92/11 to multiple environmental factors, we employed dilute
129 batch cultures, investigated its growth, POC and PIC quotas, maximum (F_v / F_m) and
130 effective photochemical quantum yield ($F_v^{'} / F_m^{'}$) and electron transport rate (*ETR*) at
131 different levels of CO_2, light, dissolved inorganic nitrogen (DIN) and phosphate
132 concentrations (DIP).

133

Biogeosciences Discuss., https://doi.org/10.5194/bg-2018-11
Manuscript under review for journal Biogeosciences
Discussion started: 16 January 2018

2 Materials and methods

2.1 Experimental design

Emiliania huxleyi strain PML B92/11, one of the most commonly used strain in studies of *E. huxleyi*, was obtained from the culture collection at Plymouth. *E. huxleyi* was grown in diluted batch cultures (final cell concentrations were 20,000 to 130,000 cells mL^{-1}) at 20 ^{o}C in a GXZ light chamber (Dongnan Instrument Company) under a 12 : 12 h light : dark cycle (light period: 8:00 a.m. to 8:00 p.m.). The synthetic seawater medium Aquil was prepared according to Sunda et al. (2005), added by 2200 μmol L^{-1} bicarbonate (as opposed to 2380 μmol L^{-1} in the original recipe), in order to reflect the alkalinity in the South and East China Seas of about 2200 μmol L^{-1} (Chou et al., 2005; Qu et al., 2017). Initial dissolved inorganic nitrogen (DIN) and phosphate (DIP) concentrations in Aquil were 100 μmol L^{-1} and 10 μmol L^{-1}, respectively (HNHP). For Aquil medium with low DIN concentration (LN), the synthetic seawater contained 8 μmol L^{-1} NO_3^- and 10 μmol L^{-1} PO_4^{3-}, respectively. For low DIP treatment (LP), it had 100 μmol L^{-1} NO_3^- and 0.4 μmol L^{-1} PO_4^{3-}.

Under each nutrient level, the Aquil media were aerated for 24 h at 20 ^{o}C (PVDF 0.22 μm pore size, simplepure, Haining) with air containing 400 μatm or 1000 μatm pCO_2. The dry air/CO_2 mixture was humidified with double distilled water prior to the aeration to minimize evaporation. Then, the Aquil was sterilized by filtration (0.22 μm pore size, Polycap 75 AS, Whatman) and carefully pumped into autoclaved 500 mL polycarbonate bottles (Nalgene). The bottles were filled with Aquil leaving about 10

Biogeosciences Discuss., https://doi.org/10.5194/bg-2018-11
Manuscript under review for journal Biogeosciences
Discussion started: 16 January 2018

156 ml headspace to minimize gas exchange. Carbonate chemistry parameters (total
157 alkalinity (TA) and pH) were measured at the beginning and end of the experiment.
158 20 bottles at each pCO_2 level were incubated at light intensities of 80, 120, 200,
159 320, and 480 μmol photons m^{-2} s^{-1} of photosynthetically active radiation (PAR) (4
160 replicates each) measured using a PAR Detector (PMA 2132, Solar Light Company,
161 Glenside). A flow chart for the experimental treatments is presented in Fig. S1. For
162 the dilute batch cultures, initial cell concentration was 200 cells mL^{-1} and cells were
163 acclimated to the experimental treatments for at least 14 generations before starting
164 the experiment (6 days at 80 μmol photons m^{-2} s^{-1}, 5 days at 120 μmol photons m^{-2}
165 s^{-1}, and 4 days at 200–480 μmol photons m^{-2} s^{-1} at all nutrient conditions). Bottles
166 were rotated two times per day at 10:00 a.m. and 6:00 p.m. to make the cells can
167 obtain light homogeniously. To minimize changes in carbonate chemistry, final cell
168 concentrations were lower than 130,000 cells mL^{-1}, and changes in dissolved
169 inorganic carbon (DIC) concentrations were less than 10% (0.5%–9.1%).
170
171 **2.2 Nutrient concentrations, total alkalinity and pH_T measurements**
172 Sampling started at 10:30 a.m. and finished at 12:00 a.m.. 50 mL samples for
173 determination of inorganic nitrogen and phosphate concentrations were
174 syringe-filtered (0.22 μm pore size, Haining) and measured using a scanning
175 spectrophotometer (Du 800, Beckman Coulter) according to Hansen and Koroleff
176 (1999).
177 Carbonate chemistry parameters were calculated from total alkalinity (TA) and pH_T

Biogeosciences Discuss., https://doi.org/10.5194/bg-2018-11
Manuscript under review for journal Biogeosciences
Discussion started: 16 January 2018

(total scale), phosphate, temperature, and salinity using the CO_2 System (Pierrot et al., 2006). In the final days of incubation, 25 mL samples for TA measurements were filtered (0.22 μm pore size, Syringe Filter) by gentle pressure with 200 mbar and stored at 4 ^{o}C for a maximum of 7 days. TA was measured at 20 ^{o}C by potentiometric titration (AS-ALK1+, Apollo SciTech) according to Dickson et al. 2003. Samples for pH_T measurements were syringe-filtered (0.22 μm pore size), and the bottles were filled with overflow and closed immediately. The pH_T was measured at 20 ^{o}C with a pH meter (Benchtop pH, Orion 8102BN) calibrated with an equimolal pH buffer (Tris •HCl, Hanna) for sea water media (Dickson, 1993). Carbonic acid constants K_1 and K_2 were calculated according to Roy et al. (1993).

2.3 Measurements of photochemical parameters

The effective photochemical quantum yield ($F_v^{'}/F_m^{'}$) and maximum photochemical quantum yield (F_v / F_m) of photosystem II (PSII) were assessed using a XE-PAM (Walz, Germany) at 1:00 p.m.. 3 ml samples were taken from the incubation bottles, and $F_v^{'}/F_m^{'}$ values were measured immediately at active light intensities similar to the incubation light levels. 3 mL samples were kept darkly for 15 min at 20 ^{o}C, and F_v / F_m values were determined at a measuring light intensity of 0.3 μmol photons m^{-2} s^{-1} and a saturation pulse of 0.8 s at light intensity of 5000 μmol photons m^{-2} s^{-1}.

For electron transport rate (*ETR*) measurements, PAR levels were set between 1 μmol photons m^{-2} s^{-1} and 1600 μmol photons m^{-2} s^{-1} with 9 steps of 45 s each. The *ETR* (mol e^- g^{-1} Chl *a* h^{-1}) was calculated according Dimier et al. (2009), *ETR* =

200 $(F_v^{'} / F_m^{'}) \times \mathrm{PAR} \times 0.5 \times A$, where A represent the cellular absorption value normalized
201 to Chl *a*, 0.5 implicits that 50% quanta of the absorbed PAR are distributed to PSII
202 (Dimier et al., 2009). Original A value was about 2.47×10^{-7} μmol e^- $cell^{-1}$ s^{-1} and
203 normalized A value was about 8.40×10^{-3} mol e^- g^{-1} Chl *a* h^{-1}. Photosynthetic
204 response to irradiance (P-I curves) were analyzed according to Jasby and Platt (1976):
205 $ETR = ETR_{max} \times \tanh(alpha \times \mathrm{PAR} / ETR_{max})$, where ETR_{max} represents
206 light-saturated *ETR*, and *alpha* is the slop of the P-I curve at limiting irradiance, I_k
207 calculated from the expression ETR_{max} / *alpha* and represents the onset of light
208 saturation.
209
210 **2.4 Cell density measurements**
211 At the end of the incubation, about 25 ml samples were taken from the incubation
212 bottles at about 2:30 p.m.. Cell densities were measured by using a Particle Counter
213 (Beckman). Growth rate (μ) was calculated according to the equation: $\mu = (\ln N_1 - \ln$
214 $N_0) / d$, where N_0 is 200 cells mL^{-1} and N_1 is the cell concentration in the final days of
215 experiment, and *d* is the growth time span in days.
216
217 **2.5 Particulate organic (POC) and inorganic carbon (PIC) measurements**
218 GF/F filters, pre-combusted at 450 ^oC for 8 h, were used to filter the samples of total
219 particulate carbon (TPC) and particulate organic carbon (POC). TPC and POC
220 samples were stored darkly at –20^oC. For POC measurements, samples were fumed
221 with HCl for 12 h to remove inorganic carbon, and samples for TPC measurements

Biogeosciences Discuss., https://doi.org/10.5194/bg-2018-11
Manuscript under review for journal Biogeosciences
Discussion started: 16 January 2018

were not treated with HCl. All samples were dried at 60 ^{o}C for 12 h, and analyzed using a Perkin Elmer Series II CHNS/O Analyzer 2400 instrument (Perkin Elmer Waltham, MA). Particulate inorganic carbon (PIC) quota was calculated as the variance between TPC quota and POC quota. POC and PIC production rates were calculated by multiplying their contents with μ (d^{-1}), respectively.

2.6 Data analysis

Responses of growth rates, POC and PIC quotas, PIC:POC ratio, POC and PIC production rates to incubation light intensities were fitted using the model provided by Eilers and Peeters (1988): $y = \frac{PAR}{a \times PAR^2 + b \times PAR + c}$, where the parameters *a*, *b* and *c* are fitted in a least square manner. The apparent light use efficiency, the slope (α), for each light response curve was estimated as $\alpha = 1/c$.

A three-way ANOVA was used to determine the main effect of dissolved inorganic nitrate (or phosphate), pCO_2, light intensity and their interactions for these variables. A three-way ANOVA was performed to compare the fitted α between growth, POC and PIC production rates at low and high CO_2 levels under different nutrient conditions. When necessary, a Tukey Post hoc test was used to identify the differences between two CO_2, nitrate (or phosphate) or light levels. A Shapiro-Wilk's test was conducted to test residual normality and a Levene test was used to test for variance homogeneity of significant data. Statistical analysis was conducted by using R and significant level was set at $p < 0.05$.

Biogeosciences Discuss., https://doi.org/10.5194/bg-2018-11
Manuscript under review for journal Biogeosciences
Discussion started: 16 January 2018

3 Results

3.1 Dissolved inorganic nitrogen and phosphate concentrations, and carbonate chemistry paremeters

At the HNHP condition, dissolved inorganic nitrogen (DIN) and phosphate (DIP) concentrations were 101 ± 1.1 μmol L^{-1} and 10.5 ± 0.2 μmol L^{-1}, respectively, at the beginning of the experiments, and were 92.8 ± 1.6 μmol L^{-1} and 9.7 ± 0.2 μmol L^{-1} in the final days of the experiment (Table S1). At the LN condition, DIN concentrations were 8.8 ± 0.1 μmol L^{-1} at the beginning of the experiment and 1.0 ± 0.4 μmol L^{-1} at the end of the experiment. In the LP treatment, DIP concentrations were 0.4 ± 0.1 μmol L^{-1} at the beginning of the experiment, and below the detection limit (< 0.04 μmol L^{-1}) at the end of the experiment.

The carbonate system parameters (mean values for the beginning and end of incubations) are shown in Table 1. For low CO_2 (LC) condition, the pCO_2 levels of the media were about 435 μatm at HNHP, 410 μatm at LN and 370 μatm under LP conditions, and the pH_T values (reported on the total scale) were about 8.10 at HNHP, 8.11 at LN and 8.16 at LP. For high CO_2 (HC) condition, the pCO_2 levels of the media were about 970 μatm at HNHP, 935 μatm at LN and 850 μatm at LP, and the pH_T values were about 7.80 at HNHP, 7.80 at LN, and 7.85 at LP conditions. Average pCO_2 levels for all LC conditions were 410 μatm, and for all HC conditions were 925 μatm.

Biogeosciences Discuss., https://doi.org/10.5194/bg-2018-11
Manuscript under review for journal Biogeosciences
Discussion started: 16 January 2018

3.2 Growth rate

Under each nutrient condition, at both LC and HC, growth rates of *E. huxleyi* increased with elevated light intensity up to 200 μmol photons m^{-2} s^{-1} and significantly declined thereafter (Three-way ANOVA; Tukey Post hoc, all df = 2, all $p < 0.001$) (Fig. 1; Table 2). Compared with LC, growth rates at HC were 2%–7% lower at HNHP ($p < 0.05$), 5%–9% lower at LN ($p < 0.01$) and 3%–24% lower at LP ($p < 0.01$), respectively (Table 3). Under LP treatment, HC-induced reduction of growth rate was larger at higher light levels (Fig. 1c).

At LC, growth rate at LN was similar with that at HNHP under limited light intensity with 80 μmol photons m^{-2} s^{-1} (df = 1, $p = 0.82$), and significantly lower than at HNHP under optimal and supra-optimal light intensities (both df = 1, $p < 0.01$ for 200 treatment; $p = 0.005$ for 480 treatment). At HC, growth rates at LN were significantly lower than those at HNHP under limited, optimal and supra-optimal light intensities (all df = 1, $p < 0.01$ for 80, 200, 480 treatments).

At LC and at 80 μmol photons m^{-2} s^{-1}, growth rate at LP was lower than at HNHP (df = 1, $p < 0.001$); while at 120–480 μmol photons m^{-2} s^{-1}, growth rates were no significant differences between LP and HNHP (all df = 1, all $p > 0.1$) (Fig. 1; Table 3). At HC and at 80, 120 and 480 μmol photons m^{-2} s^{-1}, growth rates were significantly lower at LP than at HNHP; at 200 and 320 μmol photons m^{-2} s^{-1}, growth rates were not significantly different between LP and HNHP (both df = 1, both $p > 0.05$).

3.3 POC quota

Biogeosciences Discuss., https://doi.org/10.5194/bg-2018-11
Manuscript under review for journal Biogeosciences
Discussion started: 16 January 2018

288 Under HNHP or LP conditions, at LC, POC quotas were not significantly different
289 among 80, 120 and 200 μmol photons m^{-2} s^{-1} and increased with increased light
290 intensity from 200 to 480 μmol photons m^{-2} s^{-1} (Three-way ANOVA; Tukey Post hoc,
291 both df = 1, both $p < 0.01$); while at HC, POC quotas increased with elevated light
292 intensity up to 480 μmol photons m^{-2} s^{-1} (Fig. 2a,c; Tables 2; 3). At LN, at both LC
293 and HC, POC quotas at 320 μmol photons m^{-2} s^{-1} were significantly larger than at
294 other light intensities (Fig. 2b).

295 At HNHP or at LN, POC quotas did not show significant differences between HC
296 and LC (Fig. 2a,b). At LP, at 80 μmol photons m^{-2} s^{-1}, POC quotas were significantly
297 larger at LC than at HC (df = 1, $p = 0.003$), while at 480 μmol photons m^{-2} s^{-1}, they
298 were lower (df = 1, $p = 0.001$).

299 At both LC and HC, POC quotas were not significantly different between LN and
300 HNHP at 80–320 μmol photons m^{-2} s^{-1}, while they were lower at LN than at HNHP at
301 480 μmol photons m^{-2} s^{-1} ($p < 0.01$). At both LC and HC, POC quotas were not
302 significantly different between LP and HNHP at 80–480 μmol photons m^{-2} s^{-1} (all df
303 = 1, all $p > 0.05$).

304

305 **3.4 PIC quota**

306 At HNHP or at LN, under either LC or HC, PIC quotas increased with increasing light
307 intensity until 320 μmol photons m^{-2} s^{-1} (Three-way ANOVA; Tukey Post hoc, all df
308 = 1, all $p < 0.001$) and then leveled off with further increasing light intensity (Fig.
309 2d,e; Tables 2; 3). At LP under LC conditions, PIC quotas increased significantly

when light intensity increased from 80 to 200 μmol photons m^{-2} s^{-1} and significantly declined thereafter (both df = 1, both $p < 0.001$) (Fig. 2f), while at LP and HC, there were no significant differences among the light levels (all $p > 0.05$).

At HNHP or at LN, PIC quotas were larger at LC than at HC (all df = 1, all $p > 0.05$ at 80, 120, 200 treatments; both $p < 0.01$ at 320 and 480 treatments) (Fig. 2d,e). Under LP conditions at 200 and 320 μmol photons m^{-2} s^{-1}, PIC quotas were larger at LC than at HC (both df = 1, both $p < 0.05$) (Fig. 2f).

At both LC and HC, PIC quotas were larger at LN than at HNHP (all df = 1, all $p > 0.05$ at 80 treatment; $p < 0.05$ at 120–480 treatments) (Fig. 2d,e). For both LC and HC conditions at 80–200 μmol photons m^{-2} s^{-1}, PIC quotas were larger at LP than at HNHP (all df = 1, all $p < 0.05$), while at 320 and 480 μmol photons m^{-2} s^{-1}, they were not significantly different between LP and HNHP (Fig. 2f).

3.5 PIC:POC ratio

At HNHP under LC, PIC:POC ratio increased with elevated light intensity until 320 μmol photons m^{-2} s^{-1} and significantly declined thereafter (Three way ANOVA, Tukey Post hoc, df = 1, $p < 0.05$) (Fig. 2g; Tables 2; 3), while at HC, they were not significantly different between light treatments (all $p > 0.05$). At LN in both LC and HC treatments, PIC:POC ratio increased when light intensity increased from 80 to 200 μmol photons m^{-2} s^{-1} and were not significantly different between 200, 320 and 480 μmol photons m^{-2} s^{-1} (Fig. 2h). At LP under LC conditions, PIC:POC ratio increased with increasing light intensity until 200 μmol photons m^{-2} s^{-1}, and declined

Biogeosciences Discuss., https://doi.org/10.5194/bg-2018-11
Manuscript under review for journal Biogeosciences
Discussion started: 16 January 2018

with further increasing light intensity (both df = 1, both $p < 0.05$) (Fig. 2i), while at HC, they were not significantly different between light treatments (df = 4, $p > 0.05$).

At either HNHP or at LP, at light levels of 80–480 μmol photons m^{-2} s^{-1}, PIC:POC ratio were not significantly different between LC and HC (all df = 1, all $p > 0.05$) (Fig. 2g,i). At LN under 320 and 480 μmol photons m^{-2} s^{-1}, PIC:POC ratios were larger at LC than at HC (both df = 1, both $p < 0.05$) (Fig. 2h).

At both LC and HC, under 80–480 μmol photons m^{-2} s^{-1} PIC:POC ratios were larger at LN than at HNHP (all df = 1, $p > 0.05$ at the 80 treatment; $p < 0.05$ at the 120 to 480 treatments) (Fig. 2g,h). In both LC and HC conditions, at 80–200 μmol photons m^{-2} s^{-1} PIC:POC ratios were larger at LP than at HNHP (all df = 1, all $p < 0.05$) (Fig 2g,i), while at 320 and 480 μmol photons m^{-2} s^{-1}, they were not significantly different between LP and HNHP.

3.6 F_v/F_m and F_v'/F_m'

F_v/F_m and F_v'/F_m' showed the same patterns (Fig. 3). At each nutrient condition, at both LC and at HC, F_v/F_m and F_v'/F_m' decreased with elevated light intensity until 480 μmol photons m^{-2} s^{-1} (Three way ANOVA; Tukey Post hoc, all df = 1, all $p < 0.01$) (Fig. 3a–f; Tables 2; 3).

At either HNHP or LP, only at 480 μmol photons m^{-2} s^{-1} F_v/F_m values were significantly larger at LC than at HC (both df = 1, both $p < 0.01$) (Fig. 3a,c). At LN in the light range of 80–480 μmol photons m^{-2} s^{-1}, F_v/F_m values were not significantly different between LC and HC (all df = 1, all $p > 0.05$) (Fig. 3b).

At both LC and HC, from 80 to 480 μmol photons m^{-2} s^{-1} F_v/F_m did not show

Biogeosciences Discuss., https://doi.org/10.5194/bg-2018-11
Manuscript under review for journal Biogeosciences
Discussion started: 16 January 2018

355 significant differences between LN and HNHP (all df = 1, all $p > 0.05$), and at 480
356 μmol photons m^{-2} s^{-1}, they were lower at LP than at HNHP (both df = 1, both $p < 0.05$)
357 (Fig. 3a,c).

358 At HNHP from 80 to 480 μmol photons m^{-2} s^{-1}, F_v'/F_m' values were similar
359 between LC and HC (all df = 1, all $p > 0.05$) (Fig. 3d). At LN under 200 μmol
360 photons m^{-2} s^{-1}, and at LP under 480 μmol photons m^{-2} s^{-1}, F_v'/F_m' values were
361 larger at LC than at HC (both df = 1, both $p < 0.01$) (Fig. 3e,f).

362 At LC under 200 μmol photons m^{-2} s^{-1}, F_v'/F_m' values were significantly larger at
363 LN than at HNHP, as well as at LP compared to HNHP (both df = 1, both $p < 0.05$)
364 (Fig. 3d,e,f). At HC under 480 μmol photons m^{-2} s^{-1} F_v'/F_m' values were
365 significantly lower at LP than at HNHP (df = 1, $p < 0.01$) (Fig. 3d,f).

366

367 **3.7 ETR_{max}**

368 At HNHP and at LC, ETR_{max} increased significantly with increasing light intensities
369 until 200 μmol photons m^{-2} s^{-1} (df = 1, $p < 0.01$), and leveled off with further
370 increasing light intensities (Fig. 3g; Tables 2; 3). At HNHP and at HC, with light
371 intensities increasing from 80 to 120 μmol photons m^{-2} s^{-1}, ETR_{max} increased
372 remarkably (df = 1, $p < 0.01$), and declined significantly when light intensities further
373 increased to 480 μmol photons m^{-2} s^{-1} (df = 1, $p < 0.05$). At LN or at LP, under both
374 LC and HC, ETR_{max} increased with increasing light intensities until 200 μmol photons
375 m^{-2} s^{-1} and declined thereafter (all df = 1, all $p < 0.01$) (Fig. 3h,i).

376 At HNHP and only at 480 μmol photons m^{-2} s^{-1}, ETR_{max} was lower at HC than at

LC (df =1, $p < 0.01$) (Fig. 3g; Table 3). At LN across the light range of 80–480 µmol photons m^{-2} s^{-1}, ETR_{max} values were similar between HC and LC (Fig. 3h). At LP under 320 µmol photons m^{-2} s^{-1}, ETR_{max} was larger at HC than at LC; while at 480 µmol photons m^{-2} s^{-1}, they were lower (both df =1, both $p < 0.05$) (Fig. 3i).

At both LC and HC from 80–480 µmol photons m^{-2} s^{-1}, ETR_{max} values were larger at LN than at HNHP (Tukey Post hoc, all df = 1, $p < 0.01$ for the 120, 200 and 320 treatments at LC; $p > 0.05$ for the 80 and 480 treatments at LC; $p < 0.01$ for the 80, 200, 320 and 480 treatments at HC; $p > 0.05$ for the 120 treatment at HC) (Fig. 3g,h). At LC under 80 µmol photons m^{-2} s^{-1}, ETR_{max} was lower at LP than at HNHP (df = 1, $p > 0.1$); while at 120–480 µmol photons m^{-2} s^{-1}, ETR_{max} values were larger (Tukey Post hoc, all df = 1, $p > 0.05$ for 120, 320 and 480 treatments; $p < 0.01$ for 200 treatment) (Fig. 3g,h). At HC under 80 and 120 µmol photons m^{-2} s^{-1}, ETR_{max} values were lower at LP than at HNHP (Tukey Post hoc, both df = 1, $p > 0.1$ for the 80 treatment; $p < 0.01$ for the 120 treatment), while at 200–480 µmol photons m^{-2} s^{-1}, they were larger (Tukey Post hoc, all df = 1, $p < 0.01$ for 200 and 320 treatments; $p > 0.1$ for 480 treatment).

3.8 Apparent light use efficiency (α) for growth, POC and PIC production rates

At each nutrient condition, α values of fitted curves of growth, POC and PIC production rates were not significantly different between LC and HC, with the exception of α of PIC production rate at LP (df = 1, $p < 0.05$) (Fig. 4).

At HNHP under both LC and HC, α values of fitted curves for POC and PIC

399 production rates were not significantly different, and they were significantly larger
400 than those for growth rates (both df = 1, both $p < 0.01$) (Fig. 4a). At LN under both
401 LC and HC, and at LP under LC, α values for PIC production rates were larger than
402 those for POC production rates, which were larger than those for growth rates (all df =
403 1, all $p < 0.01$) (Fig. 4b,c). At LP and HC, α values for POC and PIC production rates
404 did not show significant differences and they were larger than that for growth rates
405 (Fig. 4c).

406 At both LC and at HC, α values of fitted curves of growth rates or POC production
407 rates were not significantly different between LN and HNHP, and between LP and
408 HNHP (Fig. 4). At LC, α values for PIC production rates were lower at HNHP than at
409 LN or at LP (both df = 1, both $p < 0.01$); at HC, they were not significantly different
410 between HNHP and LP (Fig. 4).

411

412 **4 Discussion**

413

414 In this study, we investigated synergistic negative effects of low nutrient
415 concentrations and rising pCO_2 on growth rates, especially at limiting low and
416 inhibiting high light intensities. Notably, high light intensities compensated for
417 inhibition of LP on growth rates at LC. LN reduced POC quota and its sensitivity to
418 light intensity. Both LN and LP increased PIC quotas, PIC:POC ratio, and *ETR*
419 efficiency.

420

Biogeosciences Discuss., https://doi.org/10.5194/bg-2018-11
Manuscript under review for journal Biogeosciences
Discussion started: 16 January 2018

421 **4.1 Low nutrient concentrations and high pCO_2 level synergistically reduce**
422 **growth rate.**

423 Langer et al. (2013) detected that cell numbers on the fourth to sixth days during
424 cultures were in the exponential growth phase even at 3 μmol L^{-1} NO_3^- or at 0.29
425 μmol L^{-1} PO_4^{3-} with the same *E. huxleyi* strain. In addition, other *E. huxleyi* strains
426 were in the exponential phase of growth on the fourth to the seventh days in the
427 cultures with 2.5–8 μmol L^{-1} NO_3^- or at 0.4–0.55 μmol L^{-1} PO_4^{3-} (Perrin et al., 2016;
428 Rokitta et al., 2016). All parameters were measured on the fourth to the sixth days,
429 and it is most likely that cells at all treatments were sampled in the exponential
430 growth phase in this study.

431 Less energy availability limited growth rates of *E. huxleyi* at lower light intensities,
432 while reduction in growth rates at high light intensities could be related to
433 photooxidative damage or photoinhibition (Fig. 1), because high light intensity can
434 constantly damage the reaction centers of photosystem II (PSII) of *E. huxleyi* (Fig.
435 3a–f) (Ragni et al., 2008). Nevertheless, photoinhibition was not observed in electron
436 transport rate (*ETR*) of the cells grown at 480 μmol photons m^{-2} s^{-1} even exposed to
437 light intensity of 1600 μmol photons m^{-2} s^{-1} (Figs. 1 and S3). This implies that the
438 photochemical performance during a short time exposure can hardly reflect the
439 growth response. At HC, the negative effect of high $[H^+]$ on growth rate was larger
440 than positive effects of increased CO_2 and HCO_3^- concentrations, which could be
441 attributed to lower growth rates at HC than at LC (Fig. 1) (Bach et al., 2011).

442 Based on measured PON quota and cell concentration in this study (Figs. 1 and S6),
443 PON concentrations at the end of incubations were estimated to be 7.8–9.3 μmol L^{-1}

Biogeosciences Discuss., https://doi.org/10.5194/bg-2018-11
Manuscript under review for journal Biogeosciences
Discussion started: 16 January 2018

444 at different nutrient conditions (Table S1). These were closely correlated with molar
445 drawdown of dissolved inorganic nitrate (DIN) in the cultures. *E. huxleyi* appeared to
446 be a poor competitor for inorganic nitrate under low levels of nitrate availability (Fig.
447 1). Reduced levels of gene expressions and nitrate reductase (NRase) activity in *E.*
448 *huxleyi* cells grown under low nitrate could be responsible (Bruhn et al., 2010; Rouco
449 et al., 2013), thus resulting in reduced nitrate assimilation. In addition, LN
450 concentration was shown to down-regulate transcripts of genes related to synthesis of
451 amino acids, RNA polymerases and nitrogen metabolism in *E. huxleyi* (Rokitta et al.,
452 2014), which led to lower overall biosynthetic activity and decreased the growth rates
453 (Fig. 1).

454 Synergistic effects of LN and HC on growth rates indicate that these conditions
455 may inhibit cellular metabolic activity simultaneously (Fig. 1) (Sciandra et al., 2003).
456 In fact, intracellular [H^+] have been reported to be higher in HC-grown than in
457 LC-grown *E. huxleyi* cells (Suffrian et al., 2011). To transport extra H^+ out of cells, *E.*
458 *huxleyi* at HC need more transporters and energy, but LN is likely to limit the
459 synthesis of these transporters and energy supply, therefore, it exacerbated the
460 negative effects of high [H^+] on growth of *E. huxleyi* (Fig. S6) (Bruhn et al., 2010).

461 *E. huxleyi* possesses an exceptional phosphorus acquisition capacity, which could
462 allow it to dominate in phosphate-limiting environments (Dyhrman and Palenik,
463 2003). In this study, at low levels of light intensity, uptake of phosphate could be
464 energy limited, thus their growth was more inhibited at LP (Fig. 1c). Under light
465 saturation condition, relationship of growth rates of *E. huxleyi* with phosphate

Biogeosciences Discuss., https://doi.org/10.5194/bg-2018-11
Manuscript under review for journal Biogeosciences
Discussion started: 16 January 2018

concentrations indicated a very high affinity for dissolved inorganic phosphate (DIP) with 0.04 μmol L^{-1} half-saturation constant for DIP (Fig. 5). Since LP was reported to enhance expression of gene with a role in phosphorus assimilation or metabolism and synthesis of inorganic PO_4^{3-} transporters (Dyhrman et al., 2006; McKew et al., 2015; Rokitta et al., 2016), which allowed *E. huxleyi* to take up PO_4^{3-} efficiently enough, so that LP did not result in reduced growth rate at LC in this study (Fig. 1). Rokitta et al. (2016) showed that even PO_4^{3-} concentration in the culture media declined to zero (undetectable), cell number sustained to increase for 4 days, indicating that *E. huxleyi* cells could store PO_4^{3-} and use them later. Consequently, high affinity, efficient uptake and storage capacity for PO_4^{3-} in *E. huxleyi* could account for no significant differences in growth rates between LP and HNHP under LC and saturating and supra-optimal light intensities. In fact, as reported previously, higher growth rates of *E. huxleyi* at LP in comparison to HP were found during exponential growth phase in batch cultures (Rokitta et al., 2016). In natural waters, *E. huxleyi* usually starts to bloom following diatom blooms (Tyrrell and Merico, 2004). Therefore, our results also indicate that high growth rate of *E. huxleyi* at low nutrients concentrations may drive the succession of diatom to *E. huxleyi*.

Rising CO_2 was found to lead to higher phosphorous requirements for growth, carbon fixation and nitrogen uptake, and to decrease alkaline phosphate (APase) activity in *E. huxleyi* (Matthiessen et al., 2012; Rouce et al., 2013). At HC, higher phosphorous requirements may lead to lower growth rates at LP in comparison to HNHP (Fig. 1a,c). In addition, elevated CO_2 concentrations can down-regulate the

Biogeosciences Discuss., https://doi.org/10.5194/bg-2018-11
Manuscript under review for journal Biogeosciences
Discussion started: 16 January 2018

488 uptake capacity of the cells for CO_2 and/or HCO_3^- (CO_2 concentration mechanisms),
489 which could lead to less energy cost for maintaining active uptake mechanisms (Gao
490 et al., 2012), and the save energy in the HC-grown cells, consequently, might have
491 exacerbates photo-inhibition, leading to higher inhibition of the growth under LP and
492 high light intensities (Fig. 1c).
493
494 **4.2 Low dissolved inorganic nitrogen concentration and high *p*CO_2 level**
495 **synergistically reduce POC quota**
496 At LC, *E. huxleyi* mainly uses external HCO_3^- as an inorganic carbon source for
497 photosynthesis and calcification, and increasing light intensities are able to increase
498 HCO_3^- uptake rates (Kottmeier et al., 2016). This may explain why POC and PIC
499 quotas and production rates increased with increasing light intensity (Figs. 2 and S5).
500 HC down-regulates gene expression related to the HCO_3^- transporter (Rokitta et al.,
501 2012) and decreases the HCO_3^- uptake rate in *E. huxleyi* (Kottmeier et al. 2016),
502 leading to lower PIC quotas at HC than at LC (Fig. 2). Meanwhile, cells at HC can
503 increase CO_2 uptake to compensate for low-HCO_3^--uptake for photosynthetic C
504 fixation (Kottmeier et al., 2016), explaining the similar POC quotas between HC and
505 LC (Fig. 2a–c).
506 LN down regulates expression of the *rbc*L gene coding for the large subunit of the
507 ribulose-1,5-biphosphate carboxylase/oxygenase (RUBISCO) (Bruhn et al., 2010;
508 Rokitta et al., 2014). To conserve nitrogen, cells at LN prefer to shut down the
509 synthesis of RUBISCO and then reduce carbon fixation (Falkowski et al., 1989) (Fig.

2b). At HC, lower cell division rates resulted in lower POC and PIC production rates than at LC (Fig. S5).

4.3 Low nutrient concentrations facilitate calcification and maximum electron transport rates (ETR_{max})

Müller et al. (2008) found that calcification (PIC production) occurred only in the G1 cell cycle phase, and that LN or LP held cells in the G1 phase longer, which led to larger PIC quotas and calcification rates at LN or at LP than at HNHP (Figs. 2 and S5). LC and LP treatment decreased cell division rates, elongated cell cycle, and increased coccolith production of *E. huxleyi* in the darkness (Paasche and Brubak, 1994). In the present work, however, we found slightly faster cell division (growth) and identical calcification rates at LP and high light intensities (Figs. 1c, 2f and S5). LP has been shown to up-regulate the genes involved in calcium binding proteins such as the glutamic acid related to synthesize of coccolith, calcium homeostasis and transcription factor (*cmyb*) (Wahlund et al., 2004; Dyhrman et al., 2006), and facilitates the formation of cytoplasmic membrane bodies (Shemi et al., 2016). These are related to the pathways associated with production of coccoliths (Young and Henriksen, 2003) and may also be responsible for larger PIC quotas at LP.

Calcification of coccolithophores makes an important contribution to marine carbonate counter pumps in the pelagic ocean (Rost and Riebesell, 2004). Enhanced calcification of *E. huxleyi* at low nutrient concentrations implies that blooms of calcifying *E. huxleyi* diminish the potential of the oceanic CO_2 uptake compared to non-calcifying phytoplankton blooms. On the other hand, larger PIC:POC ratios

imply faster sinking rate of *E. huxleyi* cells, facilitating the export of carbon into deeper waters (Hoffmann et al., 2015).

At low light intensities, the ETR_{max} values were severely limited by low energy input. Supraoptimal light intensities have been found to significantly reduce the abundance of several proteins involved in repair and assembly of PSII, such as repair of photodamaged Psb D1 proteins in the reaction center of PSII of *E. huxleyi* (McKew et al., 2013). These suggest that high light intensity is likely to do great damage to the PSII structure and then reduce the ETR_{max}. Especially at HC, supraoptimal light intensity and saved energy from down-regulation of CCM activity synergistically decreased ETR_{max} (Fig. 3).

A previous study found that calcification can be an additional sink for electrons in *E. huxleyi* (Xu and Gao 2012). Compared with HNHP, larger ETR_{max} at LN or at LP and at saturating light intensities likely resulted from larger calcification rates (Figs. 2 and 3). On the other hand, growth, photosynthetic carbon fixation and nitrogen uptake need energy originating from electron transport (Zhang et al., 2015). At LP and at limiting levels of light intensity, lower growth, photosynthetic carbon and nitrate assimilation rates coincided with lower ETR_{max} (Figs. 1–3), implying correlations of these physiological processes.

To provide organic carbon fixed by photosynthesis to support growth and other metabolic processes, cells need to maintain larger light-use efficiency (α) for POC production rates (Fig. 4). Calcification is an energy-dependent process (Riebesell and Tortell, 2011), and increased calcification rates at low nutrient concentrations could be

555 aided by higher light-use efficiencies (Fig. 4). In addition, besides taking up inorganic
556 carbon sources and Ca^{2+} from the seawater to calcify, cells need extra energy to expel
557 H^+ generated during calcification from the cells (Jin et al., 2017), these may also
558 account for higher light-use efficiencies for PIC production rates.

559 Nutrient availability, CO_2 level and light intensity significantly interacted to affect
560 growth rate, POC and PIC quotas, F_v / F_m, F_v' / F_m' and ETR_{max} (Table 2). Obviously,
561 the question how growth, carbon fixation and calcification rates of *E. huxleyi* would
562 respond to ocean global changes needs to be examined under multiple stressors and
563 under natural environmental variations (Feng et al., 2008, 2017). In comparison to the
564 current ocean environment, under HC and HL conditions as expected in future oceans,
565 effects of LN and LP on carbon fixation of *E. huxleyi* may partly negate each other
566 (Fig.2, Table 3). Although both HC and HL reduced calcification rates of *E. huxleyi*,
567 low nutrient concentrations showed dominant positive effects on PIC quota or
568 calcification (Fig. 2d−f), suggesting that calcification of *E. huxleyi* may increase in the
569 future pelagic oceans. Our study demonstrates that complex effects of multiple
570 environmental drivers on phytoplankton require us to investigate the underlying
571 mechanisms of these interactions, in order to comprehend how ecological and
572 biogeochemical functions of key phytoplankton groups may respond to ocean global
573 changes.

574

575

576

References

Bach, L. T., Riebesell, U., and Schulz, K. G.: Distinguishing between the effects of ocean acidification and ocean carbonation in the coccolithophore *Emiliania huxleyi*, Limnol. Oceanogr., 56, 2040–2050, https://doi.org/10.4319/lo.2011.56.6.2040, 2011.

Bach, L. T., Riebesell, U., Gutowska, M. A., Federwisch, L., and Schulz, K. G.: A unifying concept of coccolithophore sensitivity to changing carbonate chemistry embedded in an ecological framework, Prog. Oceanogr., 135, 125–138, doi: 10.1016/j.pocean.2015.04.012, 2015.

Behrenfeld, M., O'Malley, R., Siegel, D., McClain, C., Sarmiento, J., Feldman, G., Milligan, A., Falkowski, P., Letelier, R., and Boss, E.: Climate-driven trends in contemporary ocean productivity, Nature, 444, 752–755, https://doi.org/10.1038/nature05317, 2006.

Borchard, C., Borges, A. V., Händel, N., and Engel, A.: Biogeochemical response of Emiliania huxleyi (PML B92/11) to elevated CO_2 and temperature under phosphorous limitation: A chemostat study, J. Exp. Mar. Biol. Ecol., 410, 61–71, https://doi.org/10.1016/j.jembe.2011.10.004, 2011.

Boyd, P. W., Dillingham, P. W., McGraw, C. M., Armstrong, E. A., Cornwall, C. E., Feng, Y. Y., Hurd, C. L., Gault-Ringold, M., Roleda, M. Y., Timmins-Schiffman, E., and Nunn, B. L.: Physiological responses of a Southern Ocean diatom to complex future ocean conditions, Nat. Clim. Change, 6, 207–213, https://doi.org/10.1038/NCLIMATE2811, 2016.

599 Brennan, G., and Colllins, S.: Growth responses of a green alga to multiple
600 environmental drivers, Nat. Clim. Change, 5, 892–897,
601 https://doi.org/10.1038/nclimate2682, 2015.
602 Bruhn, A., LaRoche, J., and Richardson, K.: *Emiliania huxleyi* (Prymnesiophyceae):
603 nitrogen-metabolism genes and their expression in response to external nitrogen
604 sources, J. Phycol., 46, 266–277, https://doi.org/10.1111/j.1529-8817.2010.00809,
605 2010.
606 Caldeira, K., and Wickett, M. E.: Oceanography: anthropogenic carbon and ocean pH,
607 Nature, 425, 365–365, https://doi.org/10.1038/425365a, 2003.
608 Chou, W. C., Sheu, D. D., Chen, C. A., Wang, S. L., and Tseng, C. M.: Seasonal
609 variability of carbon chemistry at the SEATS time-series site, Northern South
610 China Sea betweeen 2002 and 2003, Terr. Atmos. Ocean. Sci., 16, 445–465,
611 https://doi.org/10.3319/TAO.2005.16.2.445, 2005.
612 Cloern, J. E.: The relative importance of light and nutrient limitation of phytoplankton
613 growth: a simple index of coastal ecosystem sensitivity to nutrient enrichment,
614 Aquat. Ecol., 33, 3–16, https://doi.org/10.1023/A:1009952125558, 1999.
615 Dickson, A. G.: pH buffers for sea water media based on the total hydrogen ion
616 concentration scale, Deep Sea Res., 40, 107–118, 1993.
617 Dickson, A. G., Afghan, J. D., and Anderson, G. C.: Reference materials for oceanic
618 CO_2 analysis: a method for the certification of total alkalinity, Mar. Chem., 80,
619 185–197, https://doi.org/10.1016/S0304-4203(02)00133-0, 2003.
620 Dimier, C., Brunet, C., Geider, R., and Raven, J.: Growth and photoregulation

621 dynamics of the picoeukaryote *Pelagomonas calceolata* in fluctuating light,
622 Limnol. Oceanog., 54, 823–836, https://doi.org/10.4319/lo.2009.54.3.0823, 2009.
623 Dyhrman, S. T., Haley, S. T., Birkeland, S. R., Wurch, L. L., Cipriano, M. J., and
624 McArthur, A. G.: Long serial analysis of gene expression for gene discovery and
625 transcriptome profiling in the widespread marine coccolithophore *Emiliania*
626 *huxleyi*, Appl. Environ. Microb., 72, 252–260,
627 https://doi.org/10.1128/AEM.72.1.252-260.2006, 2006.
628 Dyhrman, S. T., and Palenik, B.: Characterization of ectoenzyme activity and
629 phosphate-regulated proteins in the coccolithophorid *Emiliania huxleyi*, J Plank.
630 Res., 25, 1215–1225, https://doi.org/10.1093/plankt/fbg086, 2003.
631 Eilers, P., and Peeters, J.: A model for the relationship between light intensity and the
632 rate of photosynthesis in phytoplankton, Ecol. Model., 42, 199–215,
633 https://doi.org/10.1016/0304-3800(88)90057-9, 1988.
634 Engel, A., Novoa C. C., Wurst, M., Endres, S., Tang, T., Schartau, M., Lee, C.: No
635 detectable effect of CO_2 on elemental stoichiometry of *Emiliania huxleyi* in
636 nutrient-limited, acclimated continuous cultures, Mar. Ecol. Prog. Ser., 507, 15–30,
637 https://doi.org/10.3354/meps10824, 2014.
638 Falkowski, P. G., Sukenik, A., and Herzig, R.: Nitrogen limitation in *Isochrysis*
639 *galbana* (Haptophyceae). II. Relative abundance of chloroplast proteins, J. Phycol.,
640 25, 471–478, https://doi.org/10.1111/j.1529-8817.1989.tb00252.x, 1989.
641 Feng, Y. Y., Roleda, M. Y., Armstrong, E., Boyd, P. W., and Hurd, C. L.:
642 Environmental controls on the growth, photosynthetic and calcification rates of a

643 Southern Hemisphere strain of the coccolithophore *Emiliania huxleyi*, Limnol.
644 Oceanogr, 62, 519–540, https://doi.org/10.1002/lno.10442, 2017.
645 Feng, Y. Y., Warner, M. E., Zhang, Y. H., Sun, J., Fu, F. X., Rose, J. M., and Hutchins,
646 D. A.: Interactive effects of increased pCO_2, temperature and irradiance on the
647 marine coccolithophore *Emiliania huxleyi* (Prymnesiophyceae), Europ. J. Phycol.,
648 43, 87–98, https://doi.org/10.1080/09670260701664674, 2008.
649 Gao, K. S., Xu, J. T., Gao, G., Li, Y. H., Hutchins, D. A., Huang, B. Q., Wang, L.,
650 Zheng, Y., Jin, P., Cai, X. N., Häder, D. P., Li, W., Xu, K., Liu, N. N., and
651 Riebesell, U.: Rising CO_2 and increased light exposure synergistically reduce
652 marine primary productivity, Nat. Clim. Change, 2, 519–523,
653 https://doi.org/10.1038/nclimate1507, 2012.
654 Geider, R. J., MacIntyre, H. L., and Kana, T. M.: A dynamic model of phytoplankton
655 growth and acclimation: responses of the balanced growth rate and chlorophyll *a* :
656 carbon ratio to light, nutrient-limitation and temperature, Mar. Ecol. Prog. Ser.,
657 148, 187–200, https://doi.org/10.3354/meps148187, 1997.
658 Hansen, H. P., and Koroleff, F.: Determination of nutrients, in: Methods of seawater
659 analysis, edited by: Grasshoff, K., Kremling, K., and Ehrhardt, M., WILEY-VCH
660 Publishers, 159–228, 1999.
661 Harrison, W. G., and Li, W. K. W: Phytoplankton growth and regulation in the
662 Labrador Sea: light and nutrient limitation, J. Northw. Atl. Fish. Sci., 39, 71–82,
663 https://doi.org/10.2960/J.v39.m592, 2008.
664 Hoffmann, R., Kirchlechner, C., Langer, G., Wochnik, A. S., Griesshaber, E., Schmah,

W. W., and Scheu, C.: Insight into *Emiliania huxleyi* coccospheres by focused ion beam sectioning, Biogeosciences, 12, 825–834, https://doi.org/10.5194/bg-12-825-2015, 2015.

Hutchins, D. A., and Fu, F. X.: Microorganisms and ocean global change, Nat. Microbiol., 2, 17058, https://doi.org/10.1038/nmicrobiol.2017.58, 2017.

Jasby, A. D., and Platt, T.: Mathematical formulation of the relationship between photosynthesis and light for phytoplankton, Limnol. Oceanogr., 21, 540–547, https://doi.org/10.4319/lo.1976.21.4.0540, 1976.

Jin, P., Ding, J., Xing, T., Riebesell, U., and Gao, K.: High levels of solar radiation offset impacts of ocean acidification on calcifying and non-calcifying strains of *Emiliania huxleyi*, Mar. Ecol. Prog. Ser., 568, 47–58, https://doi.org/10.3354/meps12042, 2017.

Kim, H. S., Hwang, S. J., Shin, J. K., An, K. G., and Yoon, C. G.: Effects of limiting nutrients and N:P ratios on the phytoplankton growth in a shallow hypertrophic reservoir, Hydrobiologia, 581, 255–267, https://doi.org/10.1007/s10750-007-0727-1, 2007.

Kottmeier, D. M., Rokitta, S. D., and Rost, B.: Acidification, not carbonation, is the major regulator of carbon fluxes in the coccolithophore *Emiliania huxleyi*, New Phytol., 211, 126–137, https://doi.org/10.1111/nph.13885, 2016.

Langer, G., Nehrke, G., Probert, I., Ly, J., and Ziveri, P.: Strain-specific responses of *Emiliania huxleyi* to changing seawater carbonate chemistry, Biogeosciences, 6, 2637–2646, https://doi.org/10.5194/bg-6-2637-2009, 2009.

687 Langer, G., Oetjen, K., and Brenneis, T.: Coccolithophores do not increase particulate
688 carbon production under nutrient limitation: A case study using *Emiliania huxleyi*
689 (PML92/11), J. Exp. Mar. Biol. Ecol., 443, 155–161, 2013
690 Leonardos, N., and Geider, R. J.: Eleveted atmospheric carbon dioxide increases
691 organic carbon fixation by *Emiliania huxleyi* (Haptophyta), under nutrient-limited
692 high-light conditions, J. Phycol., 41, 1196–1203,
693 https://doi.org/10.1111/j.1529-8817.2005.00152.x, 2005.
694 Matthiessen, B., Eggers, S. L., and Krug, S. A.: High nitrate to phosphorus regime
695 attenuates negative effects of rising pCO_2 on total population carbon accumulation,
696 Biogeosciences, 9, 1195–1203, https://doi.org/10.5194/bg-9-1195-2012, 2012.
697 McKew, B. A., Davey, P., Finch, S. J., Hopkins, J., Lefebvre, S. C., Metodiev, M. V.,
698 Oxborough, K., Raines, C. A., Lawso, T., and Geider, R. J.: The trade-off between
699 the light-harvesting and photoprotective functions of fucoxanthin-chlorophyll
700 proteins dominates light acclimation in *Emiliania huxleyi* (clone CCMP 1516),
701 New Phytol., 200, 74–85, https://doi.org/10.1111/nph.12373, 2013.
702 McKew, B. A., Metodieva, G., Raines, C. A., Metodier, M. V., and Geider, R. J.:
703 Acclimation of *Emiliania huxleyi* (1516) to nutrient limitation involves precise
704 modification of the proteome to scavenge alternative sources of N and P, Environ.
705 Microbiol., 17, 4050–4062, https://doi.org/10.1111/1462-2920.12957, 2015.
706 Meyer, J., and Riebesell, U.: Reviews and syntheses: Responses of coccolithophores
707 to ocean acidification: a meta-analysis, Biogeosciences, 12, 1671–1682,
708 https://doi.org/10.5194/bg-12-1671-2015, 2015.

709 Müller, M. N., Antia, A. N., and LaRoche, J.: Influence of cell cycle phase on
710 calcification in the coccolithophore *Emiliania huxleyi*, Limnol. Oceanogr., 53,
711 506–512, https://doi.org/10.4319/lo.2008.53.2.0506, 2008.
712 Müller, M. N., Trull, T. W., and Hallegraeff, G. M.: Independence of nutrient
713 limitation and carbon dioxide impacts on the Southern Ocean coccolithophore
714 *Emiliania huxleyi*, ISME J., 11, 1777–1787, https://doi.org/10.1038/ismej.2017.53,
715 2017.
716 Paasche, E., and Brubak, S.: Enhanced calcification in the coccolithophorid *Emiliania*
717 *huxleyi* (Haptophyceae) under phosphorus limitation, Phycologia, 33, 324–330,
718 1994.
719 Perrin, L., Probert, I., Langer, G., and Aloisi, G.: Growth of the coccolithophore
720 *Emiliania huxleyi* in light- and nutrient-limited batch reactors: relevance for the
721 BIOSOPE deep ecological niche of coccolithophores, Biogeosciences, 13,
722 5983–6001, https://doi,org/10.5194/bg-13-5983-2016, 2016.
723 Pierrot, D., Lewis, E., and Wallace, D. W. R.: MS Excel program developed for CO_2
724 system calculations, ORNL/CDIAC-105, Carbon Dioxide Information Analysis
725 Centre, Oak Ridge National Laboratory, U.S. Department of Energy.
726 https://doi.org/10.3334/CDIAC/otg.CO2SYS_XLS_CDIAC105a, 2006.
727 Qu, B., Song, J., Yuan, H., Li, X., Li, N., and Duan, L.: Comparison of carbonate
728 parameters and air-sea CO2 flux in the southern Yellow Sea and East China Sea
729 during spring and summer of 2011, J. Oceanogr., 73, 365–382,
730 https://doi.org/10.1007/s10872-016-0409-6, 2017.

731 Ragni, M., Airs, R. L., Leonardos, N., and Geider, R. J.: Photoinhibition of PSII in
732 *Emiliania huxleyi* (Haptophyta) under high light stress: the roles of
733 photoacclimation, photoprotection, and photorepair, J. Phycol., 44, 670–683,
734 https://doi.org/10.1111/j.1529-8817.2008.00524.x, 2008.
735 Richier, S., Fiorini, S., Kerros, M. E., Von Dassow, P., and Gattuso, J. P.: Response of
736 the calcifying coccolithophore *Emiliania huxleyi* to low pH/high pCO_2: from
737 physiology to molecular level, Mar. Biol., 158, 551–560,
738 https://doi.org/10.1007/s00227-010-1580-8, 2011.
739 Riebesell, U., and Tortell, P. D.: Effects of ocean acidification on pelagic organisms
740 and ecosystems, in: Ocean acidification, edited by: Gattuso, J. P., and Hansson, L.,
741 Oxford University Press, 99–121, 2011.
742 Riegman, R., Stolte, W., Noordeloos, A. A. M., and Slezak, D.: Nutrient uptake and
743 alkaline phosphatase (EC3:1:3:1) activity of *Emiliania huxleyi*
744 (Prymnesiophyceae) during growth under N and P limitation in continuous
745 cultures, J. Phycol., 36, 87–96, https://doi.org/10.1046/j.1529-8817.2000.99023.x,
746 2000.
747 Rokitta, S. D., John, U., and Rost, B.: Ocean acidification affects redox-balance and
748 ion-homeostasis in the life-cycle stages of *Emiliania huxleyi*, PLOS ONE, 7,
749 e52212, https://doi.org/10.1317/journal.pone.0052212, 2012.
750 Rokitta, S. D., von Dassow, P., Rost, B., and John, U.: *Emiliania huxleyi* endures
751 N-limitation with an efficient metabolic budgeting and effective ATP synthesis,
752 BMC Genomics, 15, 1051–1064, https://doi.org/10.1186/1471-2164-15-1051,

2014.

Rokitta, S. D., von Dassow, P., Rost, B., and John, U.: P- and N-depletion trigger similar cellular responses to promote senescence in eukaryotic phytoplankton, Front. Mar. Sci., 3, 109, https://doi.org/10.3389/fmars.2016.00109, 2016.

Rost, B., and Riebesell, U.: Coccolithophores and the biological pump: responses to environmental changes, in: Coccolithophores – From Molecular Biology to Global Impact, edited by: Thierstein, H. R. and Young, J. R., Springer, Berlin, 99–125, https://doi.org/10.1007/978-3-662-06278-4_52004, 2004.

Rouco, M., Branson, O., Lebrato, M., and Iglesias-Rodr ́guez, M. D.: The effect of nitrate and phosphate availability on *Emiliania huxleyi* (NZEH) physiology under different CO_2 scenarios, Front. Microbiol., 4, 155, https://doi.org/10.3389/fmicb.2013.00155, 2013.

Roy, R. N., Roy, L. N., Vogel, K. M., Porter-Moore, C., Pearson, T., Good, C. E., Millero, F. J., and Campbell, D. C.: Thermodynamics of the dissociation of boric acid in seawater at S 5 35 from 0 degrees C to 55 degrees C, Mar. Chem., 44, 243–248, 1993.

Sciandra, A., Harlay, J., Lef évre, D., Lem ée, R., Rimmelin, P., Denis, M., and Gattuso, J. P.: Response of coccolithophorid *Emiliania huxleyi* to elevated partial pressure of CO_2 under nitrogen limitation, Mar. Ecol. Prog. Ser., 261, 111–122, https://doi.org/10.3354/meps261111, 2003.

Sett, S., Bach, L. T., Schulz, K. G., Koch-Klavsen, S., Lebrato, M., and Riebesell, U.: Temperature modulates coccolithophorid sensitivity of growth, photosynthesis and

calcification to increasing seawater pCO_2, PLOS ONE, 9, e88308, https://doi.org/10.1371/journal.pone.0088308, 2014.

Shemi, A., Schatz, D., Fredricks, H. F., Van Mooy, B. A. S., Porat, Z., and Vardi, A: Phosphorus starvation induces membrane remodeling and recycling in *Emiliania huxleyi*, New Phytol., 211, 886–898, https://doi.org/10.1111/nph.13940, 2016.

Suffrian, K., Schulz, K. G., Gutowska, M., Riebesell, U., and Bleich, M.: Cellular pH measurements in *Emiliania huxleyi* reveal pronounced membrane proton permeability, New Phytol, 190, 595–608, https://doi.org/10.1111/j.1469-8137.2010.03633.x, 2011.

Sunda, W. G., Price, N. M., and Morel, F. M. M.: Trace metal ion buffers and their use in culture studies, in: Algal culturing techniques, edited by: Andersen R. A., Elsevier Academic Press, London, 53–59, 2005

Tong, S. Y., Hutchins, D. A., Fu, F. X., and Gao, K. S.: Effects of varying growth irradiance and nitrogen sources on calcification and physiological performance of the coccolithophore *Gephyrocapsa oceanica* grown under nitrogen limitation, Limnol. Oceanogr., 61, 2234–2242, https://doi.org/10.1002/lno.10371, 2016.

Tyrrell, T., and Merico, A.: *Emiliania huxleyi*: bloom observations and the conditions that induce them, in: Coccolithophores: From molecular biology to global impact, edited by: Thierstein, H. R., and Young, J. R., Springer, Berlin, 75–97, https://doi.org/10.1007/978-3-662-06278-4_4, 2004.

Wahlund, T. M., Hadaegh, A. R., Clark, R., Nguyen, B., Fanelli, M., and Read, B. A.: Analysis of expressed sequence tags from calcifying cells of marine

797 coccolithophorid (*Emiliania huxleyi*), Mar. Biotechnol., 6, 278–290,
798 https://doi.org/10.1007/s10126-003-0035-3, 2004.
799 Wang, G., Xie, S. P., Huang, R. X., and Chen, C.: Robust warming pattern of global
800 subtropical oceans and its mechanism, J. Clim., 28, 8574–8584,
801 https://doi.org/10.1175/JCLI-D-14-00809.1, 2015.
802 Xu, K., and Gao, K. S.: Reduced calcification decreases photoprotective capability in
803 the coccolithophorid *Emiliania huxleyi*, Plant Cell Physiol., 53, 1267–1274,
804 https://doi.org/10.1093/pcp/pcs066, 2012.
805 Young, J. R., and Henrikse, K.: Biomineralization within vesicles: the calcite of
806 coccoliths, Rev. Mineral. Geochem., 54, 189–215,
807 https://doi.org/10.2113/0540189, 2003.
808 Zhang, Y., Bach, L. T., Schulz, K. G., and Riebesell, U.: The modulating effect of
809 light intensity on the response of the coccolithophore *Gephyrocapsa oceanica* to
810 ocean acidification, Limnol. Oceanogr., 60, 2145–2157,
811 https://doi.org/10.1002/lno.10161, 2015.
812
813
814
815
816
817
818

819

820

821 *Competing interests*: The authors declare that they have no conflict of interest.

822

823

824 *Acknowledgements.*

825 This study was supported by National Natural Science Foundation (41720104005,
826 41430967), and Joint project of National Natural Science Foundation of China and
827 Shandong province (No. U1606404), China Postdoctoral Science Foundation
828 (2017M612129) and the outstanding postdoctoral program of State Key Laboratory of
829 Marine Environmental Science (Xiamen University). FF and DH's visits to Xiamen
830 was supported by MEL's visiting scientists program.

831

832

833

834

835

836

837

838

839

840

841 **Figure Legends**

842 **Figure 1.** Growth rate of *Emiliania huxleyi* as a function of light intensities at low
843 pCO_2 (LC) and high pCO_2 levels (HC) at high dissolved inorganic nitrogen (DIN) and
844 phosphate (DIP) concentrations (HNHP)(**a**), low DIN and high DIP concentrations
845 (LN) (**b**), or high DIN and low DIP concentrations (LP) (**c**). The solid lines in each
846 panel were fitted using the model provided by Eilers and Peeters (1988). The values
847 represent the mean ± standard deviation for four replicates.

848

849 **Figure 2.** At both LC and HC, POC quotas of *E. huxleyi* as a function of light
850 intensities at HNHP (**a**), LN (**b**) and LP (**c**) conditions. At both LC and HC, light
851 responses of PIC quotas of *E. huxleyi* at HNHP (**d**), LN (**e**) and LP (**f**) conditions. At
852 both LC and HC, light responses of PIC:POC ratios of *E. huxleyi* at HNHP (**g**), LN (**h**)
853 and LP (**i**) conditions. The solid lines in each panel were fitted using the model
854 provided by Eilers and Peeters (1988). The values represent the mean ± standard
855 deviation for four replicates.

856

857 **Figure 3.** At both LC and HC, maximum photochemical quantum yields (F_v/F_m) of *E.*
858 *huxleyi* as a function of light intensities at HNHP (**a**), LN (**b**) and LP (**c**) conditions.
859 At both LC and HC, light responses of effective photochemical quantum yields
860 (F_v'/F_m') of *E. huxleyi* at HNHP (**d**), LN (**e**) and LP (**f**) conditions. At both LC and HC,
861 light responses of fitted maximum electron transport rate (ETR_{max}) of *E. huxleyi* at
862 HNHP (**g**), LN (**h**) and LP (**i**) conditions. The values represent the mean ± standard

deviation for four replicates.

Figure 4. At both LC and HC, apparent light-use efficiency (α) for growth, POC and PIC production rates of *E. huxleyi* at HNHP (**a**), LN (**b**) and LP (**c**) conditions. α was the slope of fitted lines for growth, POC and PIC production rates. μ represents growth rate, POCpro represents POC production rate and PICpro represents PIC production rate. Different letters showed statistically difference. The values represent the mean ± standard deviation for four replicates.

Figure 5. Growth rate of *E. huxleyi* as a function of dissolved inorganic phosphate (DIP) concentrations at LC under 200 μmol photons m^{-2} s^{-1}. DIN concentration was 100 μmol L^{-1} in all culture media, and DIP concentrations were set up to 0 μmol L^{-1}, 0.25 μmol L^{-1}, 0.5 μmol L^{-1}, 1.5 μmol L^{-1}, 3 μmol L^{-1} and 10 μmol L^{-1} in the culture media. All samples were incubated at 200 μmol photons m^{-2} s^{-1} and at LC for 4 days. Solid line was fitted using the Michaelis-Menten equation. The values represent the mean ± standard deviation for four replicates.

Biogeosciences Discuss., https://doi.org/10.5194/bg-2018-11
Manuscript under review for journal Biogeosciences
Discussion started: 16 January 2018

885 **Table 1.** Carbonate chemistry parameters (mean values for the beginning and end of
886 incubations) of the media at different nutrient conditions. TA and pH samples were
887 collected and measured before and in the final days of the experiment.

	pCO_2 (µatm)	pH (total scale)	TA (µmol L^{-1})	DIC (µmol L^{-1})	HCO_3^- (µmol L^{-1})	CO_3^{2-} (µmol L^{-1})	CO_2 (µmol L^{-1})	Ω calcite
HNHP	435 ±56[a]	8.10 ±0.05[a]	2225 ±22[a]	1970 ±26[a]	1778 ±37[a]	178 ±17[a]	14 ±2[a]	4.3 ±0.4[a]
	970 ±157[b]	7.80 ±0.06[b]	2223 ±22[a]	2100 ±24[b]	1970 ±29[b]	99 ±14[b]	31 ±5[b]	2.4 ±0.3[b]
LN	410 ±52 [a]	8.11 ±0.04 [a]	2139 ±47 [a]	1888 ±60 [a]	1700 ±65 [a]	172 ±10 [a]	13 ±2 [a]	4.1 ±0.2 [a]
	936 ±143 [b]	7.80 ±0.05 [b]	2154 ±41 [a]	2034 ±55 [b]	1908 ±58 [b]	96 ±10 [b]	30 ±5 [b]	2.3 ±0.2 [b]
LP	372 ±26 [a]	8.16 ±0.02 [a]	2225 ±25 [a]	1950 ±27 [a]	1740 ±30 [a]	198 ±8 [a]	12 ±1 [a]	4.7 ±0.2 [a]
	852 ±158 [b]	7.85 ±0.06 [b]	2226 ±21 [a]	2092 ±28 [b]	1954 ±34 [b]	110 ±15 [b]	28 ±5 [b]	2.7 ±0.4 [b]

888 HNHP, 101 µmol L^{-1} dissolved inorganic nitrogen (DIN) and 10.5 µmol L^{-1} dissolved
889 inorganic phosphate (DIP); LN, 8.8 µmol L^{-1} DIN; LP, 0.4 µmol L^{-1} DIP. Different
890 letters indicate statistical difference between two pCO_2 treatments (Tukey Post hoc, p
891 < 0.01). The values are expressed as mean values ± SD calculated from measurements
892 before and in the final days of incubations.
893
894
895
896
897
898
899
900

Biogeosciences Discuss., https://doi.org/10.5194/bg-2018-11
Manuscript under review for journal Biogeosciences
Discussion started: 16 January 2018

901 **Table 2.** Results of three-way ANOVAs of the impacts of dissolved inorganic nitrate
902 (DIN) or phosphate (DIP) concentrations, pCO_2, light intensity and their interaction
903 on growth rate, POC and PIC quotas, PIC:POC ratio, F_v/F_m, F_v'/F_m' and ETR_{max}.

	Factor	*F* value	*p* value	Factor	*F* value	*p* value
Growth rate (d^{-1})	N	215.9	<0.001	P	1015.5	<0.001
	C	547.8	<0.001	C	213.3	<0.001
	L	1330.4	<0.001	L	1863.8	<0.001
	N×C	9.1	=0.004	P×C	147.6	<0.001
	N×L	11.8	<0.001	P×L	274.4	<0.001
	C×L	18.3	<0.001	C×L	11.1	<0.001
	N×C×L	4.1	=0.006	P×C×L	19.7	<0.001
POC quota	N	27.1	<0.001	P	13.7	<0.001
(pg C $cell^{-1}$)	C	0.6	=0.435	C	0.1	=0.731
	L	34.7	<0.001	L	103.2	<0.001
	N×C	13.2	<0.001	P×C	14.5	<0.001
	N×L	17.9	<0.001	P×L	0.4	=0.780
	C×L	1.0	=0.432	C×L	21.6	<0.001
	N×C×L	1.9	=0.125	P×C×L	7.3	<0.001
PIC quota	N	544.0	<0.001	P	619.1	<0.001
(pg C $cell^{-1}$)	C	70.5	<0.001	C	105.8	<0.001
	L	71.2	<0.001	L	55.3	<0.001
	N×C	2.8	=0.098	P×C	6.3	=0.015
	N×L	7.0	<0.001	P×L	9.7	<0.001
	C×L	11.4	<0.001	C×L	2.2	=0.078
	N×C×L	0.6	=0.639	P×C×L	7.0	<0.001
PIC:POC ratio	N	934.6	<0.001	P	395.0	<0.001
	C	81.8	<0.001	C	9.1	=0.004
	L	30.9	<0.001	L	47.6	<0.001
	N×C	6.6	=0.013	P×C	13.4	<0.001
	N×L	9.8	<0.001	P×L	14.4	<0.001
	C×L	6.8	<0.001	C×L	1.5	=0.202
	N×C×L	0.7	=0.567	P×C×L	4.7	=0.002
F_v/F_m	N	335.8	<0.001	P	171.2	<0.001
	C	1.5	=0.229	C	189.6	<0.001
	L	246.7	<0.001	L	153.9	<0.001
	N×C	16.1	<0.001	P×C	34.8	<0.001
	N×L	4.8	=0.002	P×L	13.8	<0.001
	C×L	12.6	<0.001	C×L	10.7	<0.001
	N×C×L	4.6	=0.003	P×C×L	2.6	=0.048
F_v'/F_m'	N	10.1	=0.002	P	675.4	<0.001
	C	33.6	<0.001	C	134.0	<0.001

	L	670.5	<0.001	L	1007.7	<0.001
	N ×C	11.7	=0.001	P ×C	195.5	<0.001
	N ×L	3.4	=0.014	P ×L	22.8	<0.001
	C ×L	14.6	<0.001	C ×L	8.2	<0.001
	N ×C ×L	12.6	<0.001	P ×C ×L	3.5	=0.012
ETR_{max}	N	811.2	<0.001	P	335.2	<0.001
(mol e^{-} g^{-1} Chl *a* h^{-1})	C	67.9	<0.001	C	71.3	<0.001
	L	176.6	<0.001	L	625.4	<0.001
	N ×C	11.2	=0.001	P ×C	20.2	<0.001
	N ×L	15.3	<0.001	P ×L	151.0	<0.001
	C ×L	4.8	=0.002	C ×L	35.1	<0.001
	N ×C ×L	12.7	<0.001	P ×C ×L	9.4	<0.001

N, dissolved inorganic nitrogen (DIN, μmol L^{-1}); P, dissolved inorganic phosphate (DIP, μmol L^{-1}); C, pCO_2 (μatm); L, light intensity (μmol photons m^{-2} s^{-1}); POC quota, particulate organic carbon content; PIC quota, particulate inorganic carbon content; F_v/F_m, maximum photochemical quantum yield; F_v'/F_m', effective photochemical quantum yield; ETR_{max}, maximum electron transport rate.

Biogeosciences Discuss., https://doi.org/10.5194/bg-2018-11
Manuscript under review for journal Biogeosciences
Discussion started: 16 January 2018

920 **Table 3.** Experimental treatments, growth rate, carbon quotas, photosynthesis

921 parameter in dilute bath cultures.

Initial N/P	pCO_2	L	Growth rate	POC quota	PIC quota	PIC: POC	F_v/F_m	F_v'/F_m'	ETR_{max}
101/ 10.5	435	80	1.11(0.02)	8.8(0.5)	1.6(0.4)	0.19(0.05)	0.59(0.01)	0.58(0.03)	1.25(0.07)
		120	1.21(0.03)	9.1(0.3)	2.3(0.7)	0.25(0.08)	0.55(0.00)	0.54(0.01)	1.52(0.12)
		200	1.37(0.02)	8.5(0.6)	2.8(0.7)	0.33(0.08)	0.55(0.01)	0.48(0.01)	1.65(0.02)
		320	1.29(0.03)	9.7(1.0)	5.0(1.3)	0.52(0.16)	0.47(0.03)	0.37(0.03)	1.58(0.09)
		480	1.17(0.03)	12.3(0.7)	3.5(0.4)	0.28(0.04)	0.45(0.06)	0.31(0.02)	1.63(0.06)
	970	80	1.06(0.01)	7.7(0.4)	0.9(0.1)	0.12(0.02)	0.58(0.01)	0.57(0.02)	1.16(0.01)
		120	1.19(0.03)	8.9(0.2)	2.2(0.4)	0.25(0.04)	0.54(0.01)	0.52(0.01)	1.69(0.16)
		200	1.32(0.01)	8.2(0.7)	2.3(0.4)	0.28(0.06)	0.53(0.01)	0.47(0.01)	1.61(0.01)
		320	1.21(0.02)	9.9(0.8)	2.9(0.7)	0.30(0.09)	0.49(0.03)	0.37(0.02)	1.60(0.09)
		480	1.16(0.01)	11.7(1.2)	1.7(0.4)	0.14(0.02)	0.33(0.03)	0.28(0.02)	1.24(0.1)
8.8/ 10.5	410	80	1.08(0.01)	7.3(0.4)	2.9(0.6)	0.39(0.09)	0.59(0.01)	0.58(0.01)	1.44(0.04)
		120	1.21(0.01)	8.4(0.4)	4.7(0.9)	0.57(0.12)	0.57(0.00)	0.55(0.01)	2.03(0.11)
		200	1.31(0.01)	8.1(0.3)	5.9(0.8)	0.74(0.08)	0.59(0.01)	0.53(0.01)	2.50(0.15)
		320	1.29(0.01)	9.9(0.4)	8.7(0.7)	0.87(0.07)	0.45(0.04)	0.37(0.04)	2.10(0.07)
		480	1.12(0.02)	7.9(0.8)	6.8(0.8)	0.87(0.17)	0.41(0.03)	0.35(0.04)	1.69(0.14)
	936	80	1.00(0.01)	7.8(0.3)	2.4(0.7)	0.31(0.11)	0.59(0.01)	0.57(0.01)	1.66(0.04)
		120	1.11(0.01)	8.9(0.5)	4.3(0.3)	0.48(0.04)	0.55(0.01)	0.54(0.02)	1.86(0.06)
		200	1.25(0.01)	8.3(0.5)	5.6(0.8)	0.68(0.09)	0.54(0.01)	0.44(0.01)	2.35(0.16)
		320	1.21(0.01)	9.7(0.2)	5.4(0.4)	0.56(0.05)	0.50(0.01)	0.41(0.03)	2.00(0.08)
		480	1.06(0.06)	7.2(1.1)	4.2(0.6)	0.54(0.06)	0.37(0.02)	0.33(0.04)	1.76(0.15)
101/ 0.4	372	80	1.00(0.02)	8.7(0.3)	3.2(0.5)	0.36(0.06)	0.59(0.01)	0.55(0.01)	1.01(0.05)
		120	1.24(0.01)	8.3(0.2)	4.2(0.4)	0.51(0.05)	0.59(0.01)	0.55(0.01)	1.58(0.04)
		200	1.39(0.01)	8.1(0.3)	5.3(0.5)	0.66(0.09)	0.56(0.01)	054(0.02)	2.10(0.06)
		320	1.31(0.02)	9.6(0.5)	4.1(0.6)	0.43(0.08)	0.47(0.02)	0.38(0.01)	1.85(0.06)
		480	1.18(0.05)	10.8(0.6)	2.7(0.5)	0.25(0.03)	0.38(0.08)	0.29(0.04)	1.61(0.18)
	852	80	0.97(0.02)	6.9(0.5)	2.6(0.4)	0.38(0.04)	0.58(0.01)	0.54(0.02)	0.91(0.03)
		120	1.08(0.01)	9.0(0.1)	3.7(0.7)	0.41(0.07)	0.55(0.01)	0.49(0.01)	1.29(0.02)
		200	1.27(0.01)	8.1(0.1)	4.0(0.3)	0.49(0.04)	0.55(0.01)	0.51(0.02)	2.16(0.07)
		320	1.22(0.01)	8.6(0.1)	3.1(0.4)	0.36(0.05)	0.47(0.03)	0.37(0.03)	2.18(0.09)
		480	0.90(0.01)	12.8(0.6)	3.5(0.6)	0.28(0.06)	0.25(0.03)	0.17(0.01)	1.21(0.09)

922 Initial N/P, the ratio of dissolved inorganic nitrogen to phosphate at the beginning of

Biogeosciences Discuss., https://doi.org/10.5194/bg-2018-11
Manuscript under review for journal Biogeosciences
Discussion started: 16 January 2018

923 experiment; L, light intensity (μmol photons m^{-2} s^{-1}). See Table 2 for detailed
924 information. Data in the brackets are the standard deviations for four replicates.
925
926
927
928
929
930
931
932
933
934
935
936
937
938
939
940
941
942
943
944

Biogeosciences Discuss., https://doi.org/10.5194/bg-2018-11
Manuscript under review for journal Biogeosciences
Discussion started: 16 January 2018

945

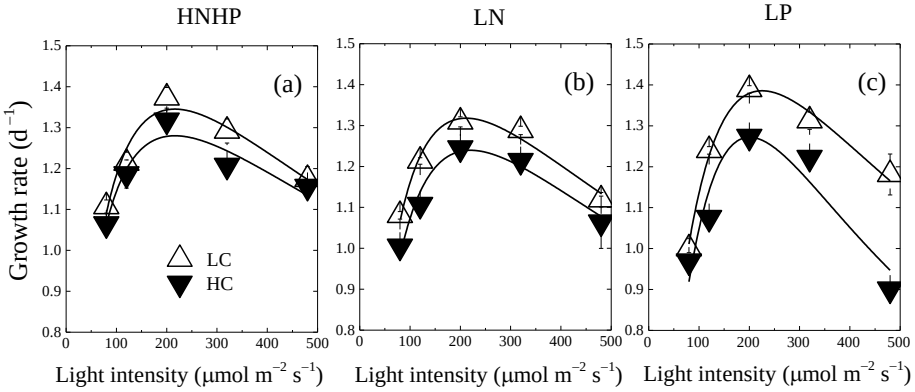

946

947

948

949

950 Figure 1

951

952

953

954

955

956

957

Biogeosciences Discuss., https://doi.org/10.5194/bg-2018-11
Manuscript under review for journal Biogeosciences
Discussion started: 16 January 2018

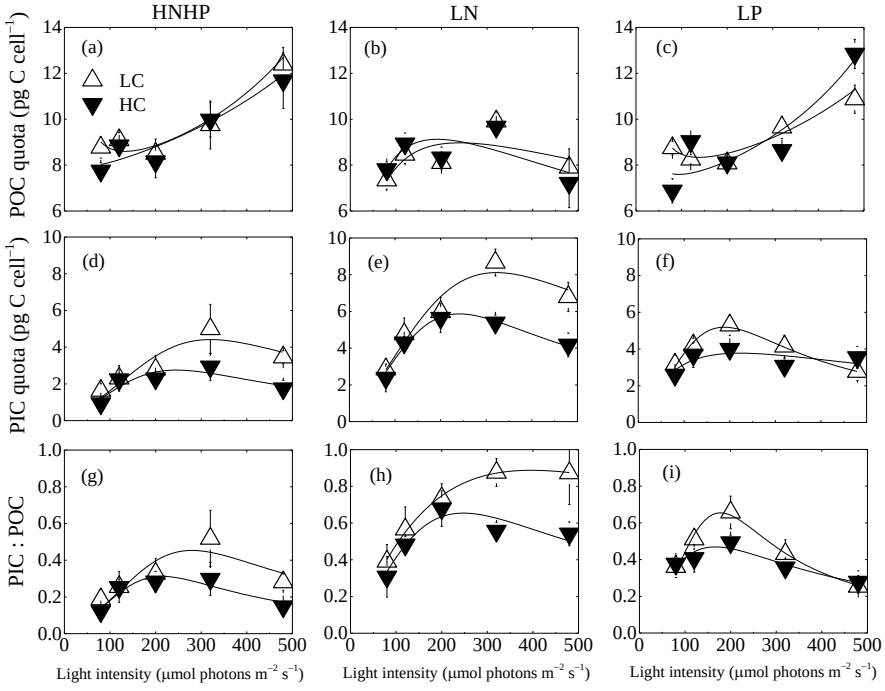

Figure 2

Biogeosciences Discuss., https://doi.org/10.5194/bg-2018-11
Manuscript under review for journal Biogeosciences
Discussion started: 16 January 2018

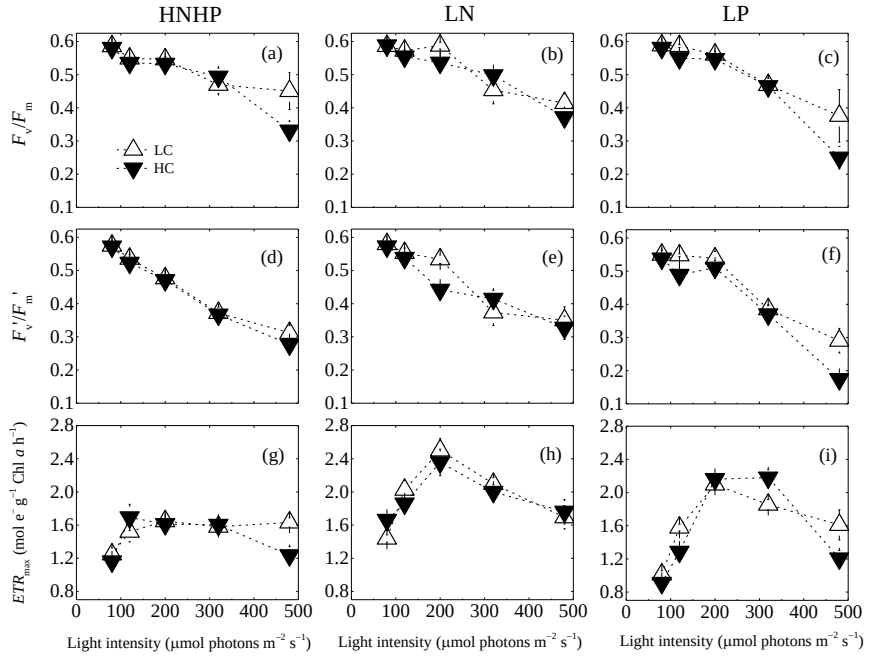

Figure 3

Biogeosciences Discuss., https://doi.org/10.5194/bg-2018-11
Manuscript under review for journal Biogeosciences
Discussion started: 16 January 2018

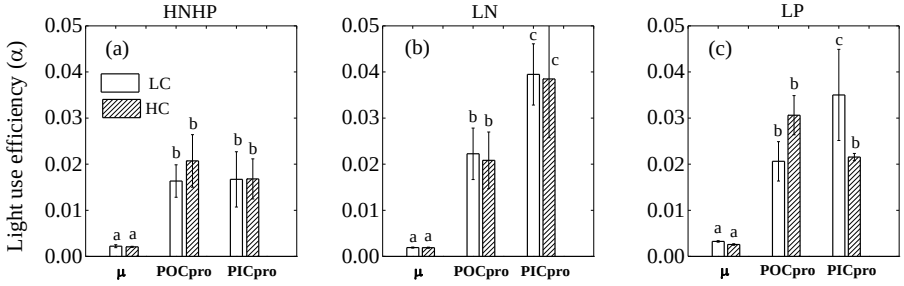

Figure 4

Biogeosciences Discuss., https://doi.org/10.5194/bg-2018-11
Manuscript under review for journal Biogeosciences
Discussion started: 16 January 2018

997

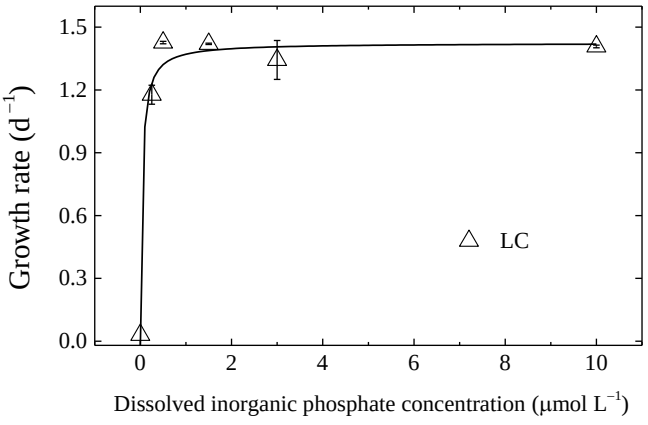

998

999

1000

1001

1002 Figure 5